

Dissection of silk glands in the Western black widow *Latrodectus hesperus*

Authors: Chaw, R. Crystal, and Hayashi, Cheryl Y.

Source: The Journal of Arachnology, 46(1) : 159-161

Published By: American Arachnological Society

URL: <https://doi.org/10.1636/JoA-16-S-063.1>

The BioOne Digital Library (<https://bioone.org/>) provides worldwide distribution for more than 580 journals and eBooks from BioOne's community of over 150 nonprofit societies, research institutions, and university presses in the biological, ecological, and environmental sciences. The BioOne Digital Library encompasses the flagship aggregation BioOne Complete (<https://bioone.org/subscribe>), the BioOne Complete Archive (<https://bioone.org/archive>), and the BioOne eBooks program offerings ESA eBook Collection (<https://bioone.org/esa-ebooks>) and CSIRO Publishing BioSelect Collection (<https://bioone.org/csiro-ebooks>).

Your use of this PDF, the BioOne Digital Library, and all posted and associated content indicates your acceptance of BioOne's Terms of Use, available at www.bioone.org/terms-of-use.

Usage of BioOne Digital Library content is strictly limited to personal, educational, and non-commercial use. Commercial inquiries or rights and permissions requests should be directed to the individual publisher as copyright holder.

BioOne is an innovative nonprofit that sees sustainable scholarly publishing as an inherently collaborative enterprise connecting authors, nonprofit publishers, academic institutions, research libraries, and research funders in the common goal of maximizing access to critical research.

SHORT COMMUNICATION

Dissection of silk glands in the Western black widow *Latrodectus hesperus*

R. Crystal Chaw^{1,2} and **Cheryl Y. Hayashi**^{1,3}: ¹Department of Evolution, Ecology and Organismal Biology, University of California at Riverside, 900 University Avenue, Riverside, California 92521, USA; E-mail: rocystalchaw@gmail.com; ²Current address: Advanced Light Microscopy Core, Department of Neurology, Oregon Health & Science University, 3181 SW Sam Jackson Park Rd., Portland, OR 97239; ³Current address: Division of Invertebrate Zoology and Sackler Institute for Comparative Genomics, American Museum of Natural History, Central Park West at 79th St. New York, NY 10024

Abstract. The silk glands of the Western black widow *Latrodectus hesperus* Chamberlin & Ivie, 1935 are morphologically and functionally distinct. Studies of spider silk glands often show only high magnification images of sections or drawings of glands, making differentiation of dissected glands difficult. We dissect all of the gland types from *L. hesperus* females and show their gross morphology with light microscopy. Our micrographs portray the distinct morphologies and relative sizes of each silk gland type, consistent with prior descriptions of the silk apparatus of *Latrodectus* spiders. Notably, we verify the presence of two differentiated pairs of aggregate silk glands and spigots, thus resolving a discrepancy in the literature.

Keywords: Theridiidae, morphology, spinneret, spigot

Black widow spiders (Theridiidae) have hundreds of silk glands. Based on morphology, these silk glands can be grouped into seven general types: aciniform, aggregate, flagelliform, major ampullate, minor ampullate, pyriform, and tubuliform (Kovoor 1987). The multiple pairs of aggregate glands can be further subdivided into “anterior” or “posterior” aggregate glands, synonymous with “typical” or “atypical” aggregate glands, respectively. Although the morphology of silk glands is used to determine silk gland identity for dissection, the gross morphology of black widow silk glands is rarely depicted; most studies show drawings of glands or sections of glands at high magnification (e.g., Kovoor 1977; Moon et al. 1998; Townley & Tillinghast 2013). The identification of black widow silk glands has become increasingly important given the growing literature on the biomechanics of widow spider silks and transcriptomics of their silk glands (e.g., Lawrence et al. 2004; Argintean et al. 2005; Garb et al. 2010; Clarke et al. 2015).

One recent study of black widows includes a video of a dissection focusing on the gross morphology of silk glands (Jeffery et al. 2011). However, some of the results of this study conflict with other descriptions of silk gland morphology for *Latrodectus* spiders (Kovoor 1977, 1987; Townley & Tillinghast 2013). Spiders that use aggregate silk glue have two pairs of aggregate silk glands (Townley & Tillinghast 2013). In theridiids, the aggregate silk gland pairs have differentiated from each other in morphology and function (Kovoor 1977, 1987). However, in their study of silk glands from black widows, Jeffery et al. (2011) identify only one pair of aggregate silk glands.

To clarify the silk gland types present in widow spiders, we reinvestigated the silk glands from the Western black widow, *Latrodectus hesperus* Chamberlin & Ivie, 1935. We documented all of the general silk gland types and their relative sizes and morphologies. Furthermore, we found two pairs of aggregate silk glands that are differentiated from each other. Our data are consistent with descriptions of theridiid silk gland types that predate the Jeffery et al. (2011) video study.

We collected adult female Western black widow *L. hesperus* spiders in June and July of 2016 (Riverside, Riverside County, CA, 33.9737° N, 117.3281° W). Spiders were anesthetized with CO₂ gas prior to dissection. Silk glands were dissected with sharpened Dumont #5 forceps in Saline Sodium Citrate (0.15 M sodium chloride, 0.015M

sodium citrate). Micrograph images of four individuals were taken through a Leica EC3 camera with Leica Application Suite (LAS) software, v. 4.6.

Seven general types of silk glands were identified: aciniform, aggregate, flagelliform, major ampullate, minor ampullate, pyriform, and tubuliform (Fig. 1). The sizes and shapes of the glands are consistent with other descriptions of theridiid silk glands. The major ampullate gland is the largest, and features a long tail that can be stretched to many mm in length (Fig. 1A; Casem et al. 2002). In comparison, the minor ampullate glands are dwarfed ampulla-shaped glands that have much shorter tails (Fig. 1B). Both major and minor ampullate glands have three parts: a tail, an ampulla-shaped storage sac, and a zig-zag duct.

Like the ampullate glands, we found two pairs of aggregate glands that are morphologically distinct from each other (Figs. 1C,D & 2C). Both pairs of aggregate glands are multi-lobed. However, the anterior aggregate gland has a wavy duct covered in a removable, nodulated sheath, while the posterior aggregate gland has a short, wide, duct that does not have a nodulated sheath (Fig. 1C,D; sheath indicated by bracket in Fig. 2C).

The long, noodle-shaped tubuliform glands are smooth and have a gradient of brown coloration that darkens toward the duct. The duct is a tight curl (Fig. 1E). We presume that the tubuliform glands are brown as a result of the silk dope; *L. hesperus* egg sacs are pale yellow to light tan and tubuliform silk is the main component of egg-case covering.

The aciniform, flagelliform, and pyriform glands are the smallest glands (Fig. 1F–H). Aciniform (Fig. 1F) and pyriform (Fig. 1G) silk glands are numerous, having multiple pairs and numbering in the hundreds, whereas only one pair of flagelliform glands (Fig. 1H) is present. Compared to the pyriform glands, the finger-like aciniform glands and ampulla-shaped flagelliform glands are larger and more easily separable. The pyriform glands are tightly associated with each other in fan-like formations that do not easily divide into individual glands (Fig. 1G). Both aciniform and pyriform silk glands have extremely fine, hair-like ducts, and neither gland type has a tail. In contrast, flagelliform glands have a distinct tail and a more robust duct (Figs. 1H & 2E).

Overall, our dissections were consistent with descriptions of theridiid silk glands (e.g., Kovoor 1977; Moon et al. 1998; Townley

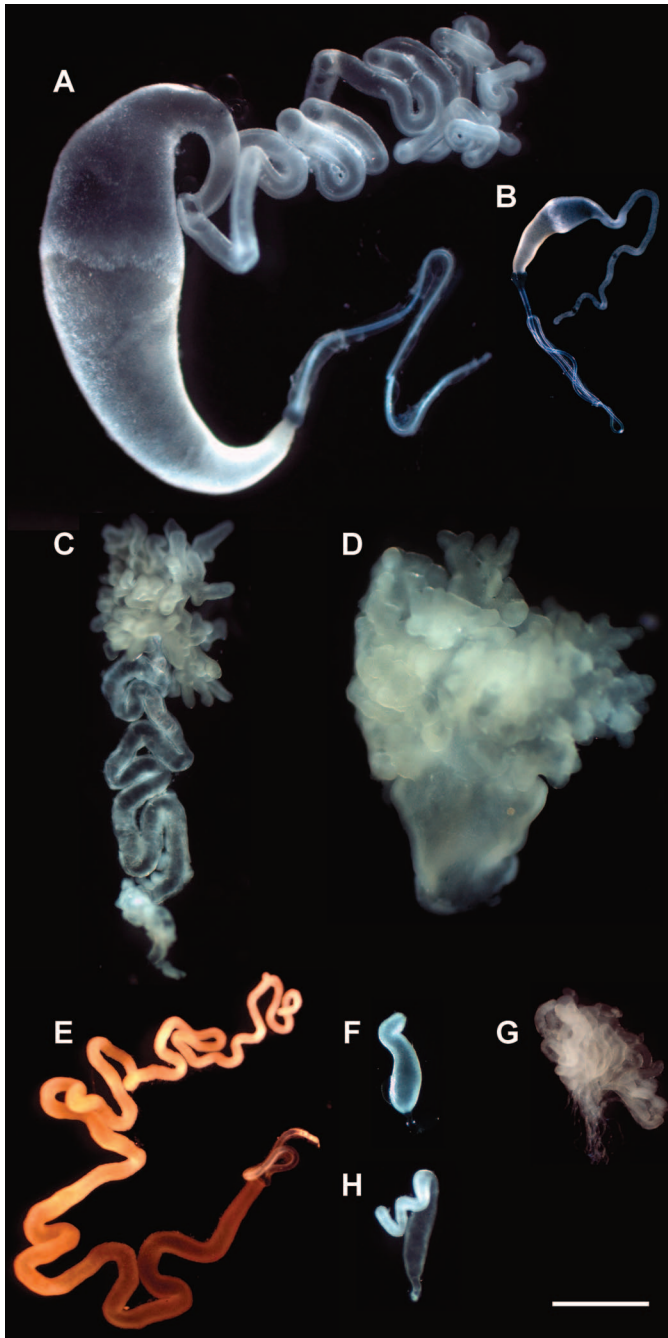


Figure 1.—Silk glands of *Latrodectus hesperus*. A. Major ampullate. Storage sac is to the left, tail (up) and duct (bottom) extend to the right. B. Minor ampullate, oriented as A. C. Anterior aggregate. Body (top) of gland is a cluster of branched lobes. D. Posterior aggregate. Body (top) of gland is lobed and globular. Duct (bottom) is wide and straight. E. Tubuliform. F. Aciniform. G. Group of approximately 20 pyriform glands. H. Flagelliform. With the exception of tubuliform, aciniform, and pyriform silk glands, all silk glands are paired in the spider and only one is depicted. There are three pairs of tubuliform glands in *L. hesperus*, a single gland is shown (E). There are hundreds of aciniform glands, and one is shown (F). Pyriform glands group into tightly associated clusters, a single cluster of approximately twenty glands is shown (G). Scale bar = 1mm.

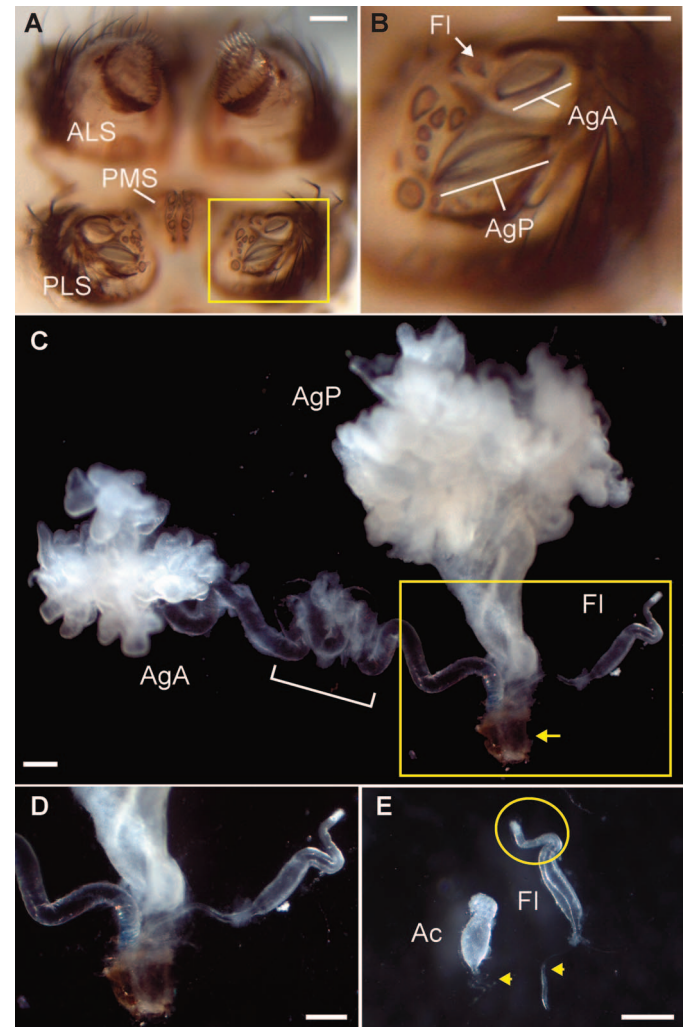


Figure 2.—A, B. Spinnerets of *Latrodectus hesperus*. A. The anterior lateral spinnerets (ALS), posterior median spinnerets (PMS) and posterior lateral spinnerets (PLS) of *Latrodectus hesperus*. Boxed area is shown in (B). B. Left posterior lateral spinneret. Flagelliform (FI), anterior aggregate (AgA) and posterior aggregate (AgP) spigots are indicated. C–E. Aggregate and flagelliform silk glands of *Latrodectus hesperus*. C. Anterior aggregate (AgA), posterior aggregate (AgP), and putative flagelliform (FI) silk glands are shown attached to the left posterior lateral spinneret. Bracket indicates nodulated area on remaining sheath. Aciniform glands have been removed for clarity. Boxed area shown in (D). D. The ducts of all three glands go to the posterior lateral spinneret. E. An aciniform silk gland (left) next to a flagelliform silk gland (right). The flagelliform silk gland has a tail (circle) and a wider duct (arrowheads) than the aciniform silk gland. Scale bars = 250 μ m.

and Tillinghast 2013). However, Jeffery et al. (2011) did not describe silk glands that match the pair of flagelliform glands that we identify. To verify our description, we looked for a triad of spigots on the posterior lateral spinnerets. Known as the aggregate and flagelliform triad, two of these spigots are relatively enormous, and one spigot is much smaller than the other two (Fig. 2A,B). This triad matches descriptions of the aggregate and flagelliform triad in the southern black widow *Latrodectus mactans* (Fabricius, 1775) by Moon et al. (1998). We found that the long, thin duct of the flagelliform gland is connected to the small spigot near the anterior of the two large, wide

spigots on the posterior lateral spinnerets (Fig. 2C,D). Although comparable in size and shape to aciniform glands, we identified the flagelliform glands by their more pronounced tails and longer, more robust ducts as compared to aciniform glands (Fig. 2E).

Based on morphology and spigot position, we propose that the silk glands defined as flagelliform and aggregate by Jeffery et al. (2011) instead correspond to the anterior and posterior aggregate silk glands of *L. hesperus*, respectively. The flagelliform glands described in the 2011 study are similar in size, shape (multi-lobed body) and duct morphology (long, wavy, nodulated) as the glands that we and other researchers have identified as anterior aggregate glands (e.g., Townley & Tillinghast 2013). Furthermore, the glands referred to as flagelliform by Jeffery et al. (2011) greatly differ from previous descriptions of theridiid flagelliform silk glands (Kovoor 1987) as well as our flagelliform glands (Fig. 1H). In our dissections, we were able to track the wavy, nodulated duct of the putative anterior aggregate silk glands to the more anterior widened spigot on the posterior lateral spinnerets. Consistently, the large, short duct of the posterior aggregate silk glands led to the larger, more posterior spigot of the aggregate/flagelliform triad (Fig. 2A,B).

We depict the gross morphology of the full complement of silk glands from *L. hesperus*. Our results resolve the conflict between a recent study of black widow silk glands (Jeffery et al. 2011) and prior descriptions of aggregate and flagelliform silk glands in theridiids (Kovoor 1977; Moon et al. 1998). Although loss of aggregate silk glands has occurred in some theridiid species, losses are accompanied by a corresponding loss of silk gland spigots (Coddington 1989; Schütt 1995; Agnarsson 2004). We confirm that *L. hesperus* spiders possess two aggregate gland spigots and one flagelliform gland spigot on each of the posterior lateral spinnerets, and we found two aggregate silk gland pairs and one flagelliform silk gland pair in *L. hesperus*. Future studies could confirm the identity of each of the glands using gene expression or biochemical methods.

ACKNOWLEDGMENTS

The authors thank Nadia Ayoub, Jonathan Coddington, and Milan Rezac for helpful discussions. This work was supported by the Army Research Office W911NF-15-1-0099 to R.C.C. and C.Y.H.

LITERATURE CITED

- Agnarsson, I. 2004. Morphological phylogeny of cobweb spiders and their relatives (Araneae, Araneoidea, Theridiidae). *Zoological Journal of the Linnean Society* 141:447–626.
- Argintean, S., J. Chen, M. Kim & A.M.F. Moore. 2005. Resilient silk captures prey in black widow cobwebs. *Applied Physics A* 82:235–241.
- Casem, M.L., L.P.P. Tran & A.M.F. Moore. 2002. Ultrastructure of the major ampullate gland of the black widow spider, *Latrodectus hesperus*. *Tissue Cell* 34:427–436.
- Chamberlin, R.V. & W. Ivie. 1935. The black widow spider and its varieties in the United States. *Bulletin of the University of Utah* 25:1–29.
- Clarke, T.H., J.E. Garb, C.Y. Hayashi, P. Arensburger & N.A. Ayoub. 2015. Spider transcriptomes identify ancient large-scale gene duplication event potentially important in silk gland evolution. *Genome Biology & Evolution* 7:1856–1870.
- Coddington, J.A. 1989. Spinneret silk spigot morphology: evidence for the monophyly of orbweaving spiders, Cyrtophorinae (Araneidae), and the group Theridiidae plus Nesticidae. *Journal of Arachnology* 17:71–95.
- Fabricius, J.C. 1775. *Systema Entomologiae, Sistens Insectorum Classes, Ordines, Genera, Species, Adiectis, Synonymis, Locis Descriptionibus Observationibus*. Flensburg and Lipsiae.
- Garb, J.E., N.A. Ayoub & C.Y. Hayashi. 2010. Untangling spider silk evolution with spidroin terminal domains. *BioMed Central Evolutionary Biology* 10:243.
- Jeffery, F., C. La Mattina, T. Tuton-Blasingame, Y. Hsia, E. Gnesa, L. Zhao et al. 2011. Microdissection of black widow spider silk-producing glands. *Journal of Visual Experiments* 47:e2382.
- Kovoor, J. 1977. Donnees histochimiques sur les glandes sericigenes de la veuve noire *Latrodectus mactans* Fabr. (Araneae, Theridiidae). *Annales des Sciences Naturelles Zoologie et Biologie Animale* 19:63–87.
- Kovoor, J. 1987. Comparative structure and histochemistry of silk-producing organs in arachnids. Pp. 160–186. *In* *Ecophysiology of Spiders*. (W. Nentwig, ed.) Springer Berlin Heidelberg.
- Lawrence, B.A., C.A. Viera & A.M.F. Moore. 2004. Molecular and mechanical properties of major ampullate silk of the black widow spider, *Latrodectus hesperus*. *Biomacromolecules* 5:689–695.
- Moon, M.J., M.A. Townley & E.K. Tillinghast. 1998. Fine structural analysis of secretory silk production in the black widow spider, *Latrodectus mactans*. *Korean Journal of Biological Sciences* 2:145–152.
- Schütt, K. 1995. *Drapetisca socialis* (Araneae: Linyphiidae): Web reduction-ethological and morphological adaptations. *European Journal of Entomology* 95:553–563.
- Townley, M.A. & E.K. Tillinghast. 2013. Aggregate silk gland secretions of araneoid spiders. Pp. 283–302. *In* *Spider Ecophysiology*. (W. Nentwig, ed.) Springer Berlin Heidelberg.

Manuscript received 23 September 2016, revised 24 July 2017.